J. FAC. SCI., SHINSHU UNIVERSITY, Vol. 30, No. 2, pp. 55-67 1995

Magnetic Phase Diagram of Bi_2CuO_4

Hideo HASHIMOTO*, Atsushi KATSUKI and Kazuko MOTIZUKI**

Department of Physics,
Faculty of Science, Shinshu University
(Received December 26, 1995)

Abstract

The ground state spin configuration in Bi_2CuO_4-type crystal having two magnetic ions in the unit cell is studied on the basis of the Heisenberg model with four kinds of superexchange interaction. The magnetic phase diagram is found to be composed of five regions : four of wich are collinear spin arrangement and one is of double helical spin arrangement. The values of exchange integrals of Bi_2CuO_4 estimated by Aïn et al from their own neutron scattering data are in the region where the observed collinear spin arrangement is stabilized.

1 Introduction

The discovery of the high temperature oxide superconductors has led to increasing interest in studies of the physical properties of CuO-based materials. Among the vast group of CuO-based materials, Bi_2CuO_4 attracts special attention because of its interesting crystal structure and magnetic properties, though Bi_2CuO_4 itself is not superconducting. The crystal structure of Bi_2CuO_4 belongs to the tetragonal space group P4/ncc. In this compound CuO_4 units, one of which consists of a square of four O ions and a Cu^{2+} ion at the centre, are stacked along the c-axis in a staggered manner, and two adjacent CuO_4 units are separated with each other by an intervening Bi cation.

The crystal structure of Bi_2CuO_4 has been determined by Attfield[1], by Ong et al[2] and by Yamada et al[3] from neutron and/or X-ray diffraction experiments. Also, the magnetic properties of this compound have been extensively studied[1-5]. Aïn et al[4] have studied the magnon dispersion relation by neutron-scattering. Furthermore, by analyzing the result on the basis of two sublattice model with four kinds of superexchange interaction, they have estimated the values of the superexchange parameters.

---

* Present adress : Faculty of Engineering, Gumma University, Kiriu 376, Japan

** Present adress : Department of Physics, Faculty of Science, Okayama University of Science, Okayama 700, Japan

The purpose of the present paper is to study theoretically what sort of spin ordering is realized in the compounds having Bi_2CuO_4-type crystal structure, on the basis of the Heisenberg model. Four kinds of isotropic superexchange interactions are assumed. We construct magnetic phase diagram as a function of the superexchange parameters and examine if the result of Aïn et al is consistent with the obtained phase diagram. In §2 the crystal structure and the sites of ions are shown. As for four kinds of superexchange interaction via -O-Bi-O- bond, each length of Cu-O, O-Bi, Bi-O, O-Cu bond, and each bond-angle of Cu-O-Bi, O-Bi-O, Bi-O-Cu are given in §2. The formulation is described in §3, and the phase diagram is shown in §4. The results are discussed and compared with the spin ordering observed in Bi_2CuO_4.

2 Crystal structure and superexchange interactions

The crystal structure and the sites of ions have been given, for example, by

Table 1. Coordinates of ions in a unit cell of Bi_2CuO_4

cation	x/a	y/a	z/c	O ion	x/a	y/a	z/c
Cu I	0.5000	0.5000	0.8420	O(I-1)	0.7005	0.6080	0.8301
				O(I-2)	0.3920	0.7005	0.8301
				O(I-3)	0.2995	0.3920	0.8301
				O(I-4)	0.6080	0.2995	0.8301
Bi(I 1 II 3)	0.6686	0.8314	0.6710				
Bi(I 4 II 2)	0.8314	0.3314	0.6710				
Bi(I 3 II 1)	0.3314	0.1686	0.6710				
Bi(I 2 II 4)	0.1686	0.6686	0.6710				
Cu II	0.0000	0.0000	0.5000	O(II-1)	0.1080	0.2005	0.5119
				O(II-2)	−0.2005	0.1080	0.5119
				O(II-3)	−0.1080	−0.2005	0.5119
				O(II-4)	0.2005	−0.1080	0.5119
Cu III	0.5000	0.5000	0.3420	O(III-1)	0.6080	0.7005	0.3301
				O(III-2)	0.2995	0.6080	0.3301
				O(III-3)	0.3920	0.2995	0.3301
				O(III-4)	0.7005	0.3920	0.3301
Bi(III 1 IV 3)	0.8314	0.6686	0.1710				
Bi(III 4 IV 2)	0.6686	0.1686	0.1710				
Bi(III 3 IV 1)	0.1686	0.3314	0.1710				
Bi(III 2 IV 4)	0.3314	0.8314	0.1710				
Cu IV	0.0000	0.0000	0.0000	O(IV-1)	0.2005	0.1080	0.0119
				O(IV-2)	−0.1080	0.2005	0.0119
				O(IV-3)	−0.2005	−0.1080	0.0119
				O(IV-4)	0.1080	−0.2005	0.0119

(According to Yamada et al,[3] $a=0.8502$nm and $c=0.5820$nm)

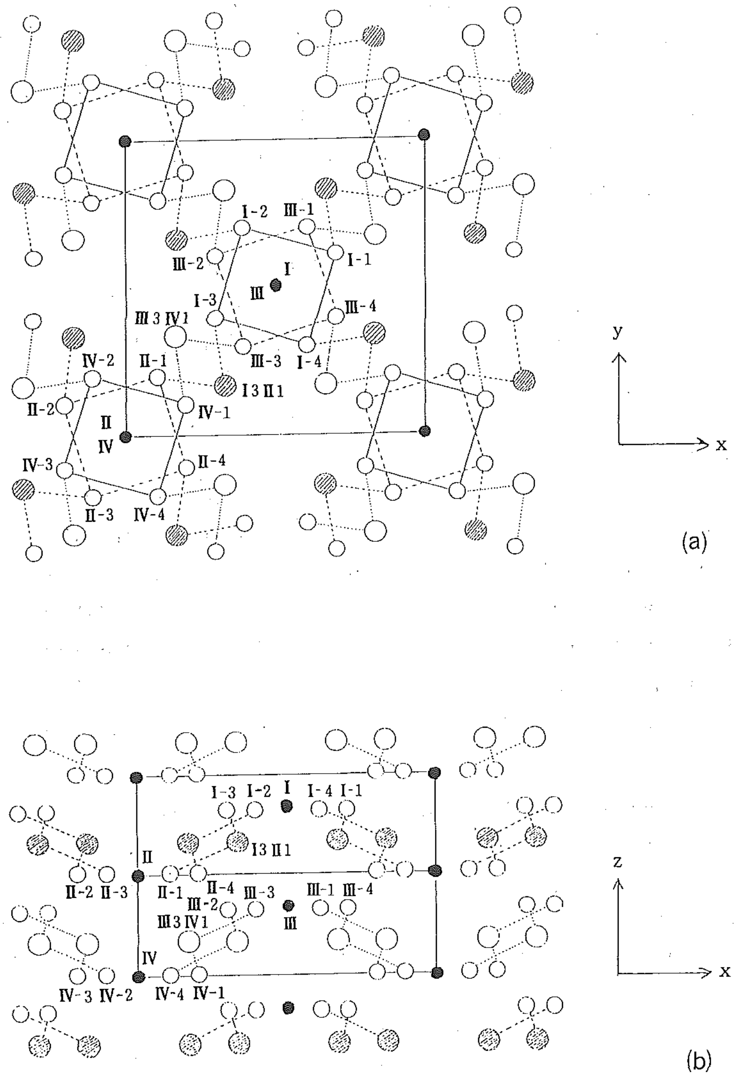

Fig. 1. Crystal structure of Bi_2CuO_4. ● : Cu ; ○ : O ; ○, ◍ : Bi
(a) Projection on *xy*-plane (b) Projection on *xz*-plane

Yamada et al[3]. A unit cell includes four Cu ions, named as Cu I , CuII, CuIII and CuIV, sixteen O ions, nemed as O(II-3), and eight Bi ions named as Bi(III3IV1). O(II-3) represents the O ion located in the third quadrant among the four O ions surrounding the CuII. Bi(III3IV1) means Bi ion whose nearest neighbouring oxygen ions are O(III-3) and O(IV-1).

Taking the position of CuⅣ to be the origin and a and c to be the lattice constants of the tetragonal lattice, we have specified the positions of ions as shown in Table 1 based on the data given by Yamada et al[3]. The projections on the xy and xz planes are shown in Fig. 1.

The sublattice consisting of the Cu ions is pseud-body centred tetragonal, CuⅣ and CuII being at coners ($z=0$ and $c/2$), and CuIII and Cu I being at positions slightly deviating from the centres along the c-axis ($z=(c/4)+\delta c$ and $(3c/4)+\delta c$, with $\delta=0.092$).

As seen from the crystal structure, of which the sublattice of Cu ions is shown in Fig. 2, there are four main types of superexchange interaction:

J_1 between Cu I ($z/c=-0.158$) and CuIII, CuⅣ and CuII, CuIII and Cu I, and CuII and CuⅣ ($z/c=1.000$),

J_2 between Cu I ($z/c=-0.158$) and CuⅣ, and CuIII and CuII,

J_3 between CuⅣ and CuIII, and CuII and Cu I, and

J_4 between Cu I ($z/c=-0.158$) and CuII, and CuIII and CuⅣ ($z/c=1.000$).

Typical paths connecting two Cu ions, between which the direct distance is shown in the spuare brackets, of these superexchange interactions are as follows:

J_1: CuⅣ—O(Ⅳ-1)—Bi(III3Ⅳ1)—O(II-1)—CuII [0.291 nm]

J_2: Cu I —O(I-3)—Bi(III3Ⅳ1)—O(Ⅳ-1)—CuⅣ [0.608 nm]

J_3: CuⅣ—O(Ⅳ-1)—Bi(III3Ⅳ1)—O(III-3)—CuIII [0.664 nm]

J_4: Cu I —O(I-3)—Bi(III3Ⅳ1)—O(II-1)—CuII [0.713 nm]

Table 2. Bond-length and bond-angles in the paths of four types of superexchange interaction

J_1	ion	CuⅣ		O(Ⅳ-1)		Bi(III3Ⅳ1)		O(II-1)		CuII
	bond-length (in nm)		0.194		0.213		0.233		0.194	
	bond-angle (Cu-O-Bi)			109.0°				119.6°		
	bond-angle (O-Bi-O)					88.5°				
J_2	ion	Cu I		O(I-3)		Bi(III3Ⅳ1)		O(Ⅳ-1)		CuⅣ
	bond-length (in nm)		0.194		0.233		0.213		0.194	
	bond-angle (Cu-O-Bi)			119.6°				109.0°		
	bond-angle (O-Bi-O)					76.5°				
J_3	ion	CuⅣ		O(Ⅳ-1)		Bi(III3Ⅳ1)		O(III-3)		CuIII
	bond-length (in nm)		0.194		0.213		0.213		0.194	
	bond-angle (Cu-O-Bi)			109.0°				109.0°		
	bond-angle (O-Bi-O)					87.8°				
J_4	ion	Cu I		O(I-3)		Bi(III3Ⅳ1)		O(II-1)		CuII
	bond-length (in nm)		0.194		0.233		0.233		0.194	
	bond-angle (Cu-O-Bi)			119.6°				119.6°		
	bond-angle (O-Bi-O)					159.1°				

From the data given in Table 1, we have estimated the bond-length and bond-angles of the four paths above as shown in Table 2.

It should be noticed that the O-Bi-O angle in J_4 is near 180° and ones in other J's are near 90° as already pointed out by Aïn et al[4]. So, we expect for J_4 to be most essential.

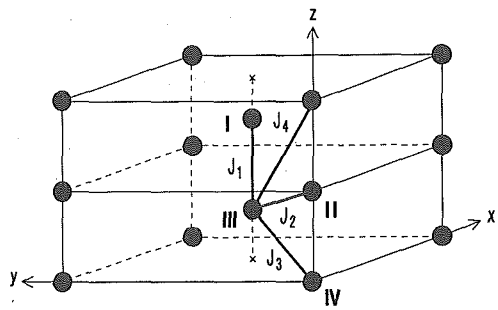

Fig. 2. Arrangement of Cu^{2+} ions and exchange interactions between them.

3 Formulation

The exchange energy E of a crystal lattice, whose unit cell contains several magnetic ions, can be written as

$$E=-\sum_{mn}\sum_{\alpha\beta}2J(R_{m\alpha,n\beta})S_{m\alpha}\cdot S_{n\beta}, \tag{1}$$

where $R_{m\alpha,n\beta}\equiv R_{m\alpha}-R_{n\beta}$, $S_{m\alpha}$ is the classical spin vector of the α-th magnetic ion in the unit cell and $R_{m\alpha}$ its position. We assume the same magnitude S for the spin vectors of all magnetic ions in the unit cell. Using the Fourier transformation of $J(R_{m\alpha,n\beta})$ and $S_{m\alpha}$

$$C_{\alpha\beta}(q)=-\sum_{m}J(R_{m\alpha,n\beta})\exp(\mathrm{i}q\cdot R_{m\alpha,n\beta}) \tag{2}$$

$$\sigma_{q\alpha}=\frac{1}{NS}\sum_{m}S_{m\alpha}\exp(-\mathrm{i}q\cdot R_{m\alpha}), \tag{3}$$

where N is the number of unit cells, eq. (1) becomes

$$\frac{E}{NS^2}=\sum_{q}\sum_{\alpha}\sum_{\beta}C_{\alpha\beta}(q)\sigma_{q\alpha}\cdot\sigma_{-q\beta}. \tag{4}$$

Our problem is to look for the lowest minimum of the exchange energy given by (4) subject to the condition

$$S_{m\alpha}{}^2=S^2 \quad \text{for all } m \text{ and } \alpha. \tag{5}$$

This condition can be written as

$$\sum_{q}\sigma_{q,\alpha}\cdot\sigma_{-q,\alpha}=1, \tag{6a}$$

$$\sum_{q}\sigma_{q,\alpha}\cdot\sigma_{q'-q,\alpha}=0 \quad \text{for all } q'\neq 0. \tag{6b}$$

Minimizing E/NS^2 of eq. (4) under the condition (6a), we have the eigenvalue equaiton:

$$\sum_{\alpha}C_{\alpha\beta}(q)\sigma_{q\alpha}=\lambda\sigma_{q\beta}, \tag{7}$$

where λ represents the Lagrange multiplier.

If we take a spin configuration represented by a pair of inequivalent wave vectors q and $-q$, namely $q\neq 0$ or $q\neq K/2$ (K being a reciprocal lattice vector), and take account of condition (6b), then we have

$$\sigma_{q\alpha}=\frac{1}{2}(\vec{i}-\mathrm{i}\vec{j})u_{q\alpha}, \tag{8}$$

where $\vec{i}$ and $\vec{j}$ are orthogonal unit vectors which are independent of α, and from eq. (6a) $|u_{q,\alpha}|=1$. When q and $-q$ are equivalent to each other, $q=0$ or $q=K/2$, $\sigma_{q\alpha}$ takes the form

$$\sigma_{q\alpha}=\vec{k}u_{q\alpha}, \tag{9}$$

where $\vec{k}$ is unit vector and $|u_{q,\alpha}|=1$. The ratio of $u_{q\alpha}$ and $u_{q\beta}$ is determined from the equation similar to (7), i.e. from

$$\sum_{\alpha} C_{\alpha\beta}(q)u_{q\alpha}=\lambda u_{q\beta}. \tag{10}$$

Now, we apply the above method to the case of Bi_2CuO_4 and discuss the spin arrangement of this compound. Two kinds of magnetic ions are contained in the unit cell and they are noted as 1 and 2. 1 represents ion at the corner corresponding to Cu_{IV} and Cu_{II} in Fig.2 and 2 that at the deviated centre corresponding to Cu_{III} and Cu_{I}. If we take into account the four types of superexchange interaction, J_1, J_2, J_3 and J_4 as shown in Fig.2, the matrix $\{C_{\alpha\beta}(q)\}$ becomes

$$\left.\begin{aligned} &C_{11}(q)=C_{22}(q)=-2J_1\cos\frac{c}{2}q_z \\ &C_{12}(q)=C_{21}{}^*(q)=-4\exp(-\mathrm{i}\delta cq_z)\cos\frac{a}{2}q_x\cos\frac{a}{2}q_y\times \\ &\qquad\times[J_2\exp(\mathrm{i}\frac{1}{4}cq_z)+J_3\exp(-\mathrm{i}\frac{1}{4}cq_z)+J_4\exp(\mathrm{i}\frac{3}{4}cq_z)] \end{aligned}\right\} \tag{11}$$

where $\delta=0.092$ and δc denotes the deviation of the position of Cu_{III} or Cu_{I} from the body centre position. In this case, the eigenvalue equation (10) is given by

$$\begin{vmatrix} C_{11}(q)-\lambda & C_{21}(q) \\ C_{12}(q) & C_{22}(q)-\lambda \end{vmatrix}=0. \tag{12}$$

By solving this equation the lower value of λ is obtained as

$$\begin{aligned} \lambda&=C_{11}(q)-|C_{12}(q)| \\ &=-2J_1\cos\frac{c}{2}q_z\mp4\cos\frac{a}{2}q_x\cos\frac{a}{2}q_y\times \\ &\qquad\times\sqrt{J_2^2+J_3^2+J_4^2+2J_2J_3\cos\frac{c}{2}q_z+2J_2J_4\cos\frac{c}{2}q_z+2J_3J_4\cos(cq_z)}. \end{aligned} \tag{13}$$

As for the double sign of eq. (13) we must take $-$ sign in the case of $\cos\frac{a}{2}q_x\cos\frac{a}{2}q_y>0$, and $+$ sign in the case of $\cos\frac{a}{2}q_x\cos\frac{a}{2}q_y<0$.

The ratio of u_{q1} and u_{q2} is determined by

$$\frac{u_{q1}}{u_{q2}}=-\frac{C_{21}(q)}{C_{11}(q)-\lambda}. \tag{14}$$

If we consider the case $q_x=q_y=0$, the ratio is given by

$$\frac{u_{q1}}{u_{q2}}=-\frac{\exp(\mathrm{i}\delta cq)\{J_2\exp(-\mathrm{i}cq/4)+J_3\exp(\mathrm{i}cq/4)+J_4\exp(-\mathrm{i}3cq/4)\}}{\sqrt{J_2^2+J_3^2+J_4^2+2J_2J_3\cos(cq/2)+2J_2J_4\cos(cq/2)+2J_3J_4\cos(cq)}}. \tag{15}$$

The spin vector of the 1st ion (Cu_{II} ion) and that of the 2nd ion (Cu_{III} ion) are respectively given by

$$\left.\begin{aligned} S_{II}&=S\sigma_{q1}\exp(\mathrm{i}q\cdot R_{II})=\frac{S}{2}u_{q1}\exp(\mathrm{i}q\cdot R_{II})\\ S_{III}&=S\sigma_{q2}\exp(\mathrm{i}q\cdot R_{III})=\frac{S}{2}u_{q2}\exp(\mathrm{i}q\cdot R_{III})\end{aligned}\right\} \tag{16}$$

Then, the relative angle θ of S_{II} and S_{III} is expressed as

$$\begin{aligned}\exp(\mathrm{i}\theta)&=\frac{S_{II}}{S_{III}}=\frac{u_{q1}}{u_{q2}}\exp\{\mathrm{i}q(R_{II}-R_{III})\}=\frac{u_{q1}}{u_{q2}}\exp\{\mathrm{i}q(\frac{1}{4}-\delta)c\}\\ &=\frac{J_2+J_3\exp(\mathrm{i}cq/2)+J_4\exp(-\mathrm{i}cq/2)}{\sqrt{J_2^2+J_3^2+J_4^2+2J_2J_3\cos(cq/2)+2J_2J_4\cos(cq/2)+2J_3J_4\cos(cq)}}.\end{aligned} \tag{17}$$

Judging from the superexchange path (see §2), we assume that J_4 is most important and negative. Then, we introduce reduced energy and reduced parameters as follows:

$$\frac{\lambda}{4|J_4|}=\varepsilon,\quad \frac{J_1}{|J_4|}=j_1,\quad \frac{J_2}{|J_4|}=j_2,\quad \frac{J_3}{|J_4|}=j_3. \tag{18}$$

The reduced energy is written as

$$\begin{aligned}\varepsilon=&-\frac{1}{2}j_1\cos\frac{c}{2}q_z\mp\cos\frac{a}{2}q_x\cos\frac{a}{2}q_y\times\\ &\times\sqrt{1+j_2^2+j_3^2-2j_2(1-j_3)\cos\frac{c}{2}q_z-2j_3\cos(cq_z)}.\end{aligned} \tag{19}$$

By differentiating ε with respect to q_x, q_y and q_z, we obtain the following relations:

$$\left.\begin{aligned}&\sin\frac{a}{2}q_x\cos\frac{a}{2}q_y\sqrt{1+j_2^2+j_3^2-2j_2(1-j_3)\cos\frac{c}{2}q_z-2j_3\cos(cq_z)}=0,\\ &\cos\frac{a}{2}q_x\sin\frac{a}{2}q_y\sqrt{1+j_2^2+j_3^2-2j_2(1-j_3)\cos\frac{c}{2}q_z-2j_3\cos(cq_z)}=0,\\ &\sin\frac{c}{2}q_z[j_1-\frac{\pm\cos(aq_x/2)\cos(aq_y/2)\times2\{j_2(1-j_3)+4j_3\cos(cq_z/2)\}}{\sqrt{1+j_2^2+j_3^2-2j_2(1-j_3)\cos(cq_z/2)-2j_3\cos(cq_z)}}]=0.\end{aligned}\right\} \tag{20}$$

The wave vector of the spin arrangement of possible stable states are obtained as $(0,0,0)$, $(0,0,2\pi/c)$, $(\pi/a,\ \pi/a,\ 0)$, $(\pi/a,\ \pi/a,\ 2\pi/c)$ and $(0,0,q)$ where q satisfies the following equation:

$$j_1=\frac{2\{j_2(1-j_3)+4j_3\cos(cq/2)\}}{\sqrt{1+j_2^2+j_3^2-2j_2(1-j_3)\cos(cq/2)-2j_3\cos(cq)}}. \tag{21}$$

The reduced exchange energy ε of these five states are given by

$$\varepsilon_1\equiv\varepsilon(0,0,0)=-\frac{1}{2}j_1-|j_2+j_3-1| \tag{22a}$$

$$\varepsilon_2=\varepsilon(0,0,2\pi/c)=\frac{1}{2}j_1-|j_2-j_3+1| \tag{22b}$$

$$\varepsilon_3=\varepsilon(\pi/a,\ \pi/a,\ 0)=-\frac{1}{2}j_1 \tag{22c}$$

$$\varepsilon_4=\varepsilon(\pi/a,\ \pi/a,\ 2\pi/c)=\frac{1}{2}j_1 \tag{22d}$$

$$\begin{aligned}\varepsilon_5&=\varepsilon(0,0,q)\\ &=-\frac{1}{2}j_1\cos\frac{c}{2}q-\sqrt{1+j_2^2+j_3^2-2j_2(1-j_3)\cos\frac{c}{2}q-2j_3\cos(cq)}\end{aligned} \tag{22e}$$

Using j_1, j_2 and j_3 defined by eq.(18), eq.(17) is written as

$$\exp(\mathrm{i}\theta)=\frac{j_2+j_3\exp(\mathrm{i}cq/2)-\exp(-\mathrm{i}cq/2)}{\sqrt{1+j_2^2+j_3^2-2j_2(1-j_3)\cos(cq/2)-2j_3\cos(cq)}}. \tag{23}$$

In the special cases of $q=(0,0,0)$ and $q=(0,0,2\pi/c)$, the relative angles θ of spin 1 and 2 are determined from the following relations:

$$\exp(\mathrm{i}\theta)=\frac{j_2+j_3-1}{\sqrt{1+j_2^2+j_3^2+2j_2j_3-2(j_2+j_3)}}=\frac{j_2+j_3-1}{|j_2+j_3-1|}\quad \text{for } q=(0,0,0) \tag{24a}$$

$$\exp(\mathrm{i}\theta)=\frac{j_2-j_3+1}{\sqrt{1+j_2^2+j_3^2-2j_2j_3+2(j_2-j_3)}}=\frac{j_2-j_3+1}{|j_2-j_3+1|}\quad \text{for } q=(0,0,2\pi/c). \tag{24b}$$

4 Phase diagram

By comparing the energy of each spin arrangement, we construct the phase diagram as a function of exchange parameterers j_1, j_2 and j_3. Apparently $\varepsilon_1<\varepsilon_3$ unless $j_2=1-j_3$, and $\varepsilon_2<\varepsilon_4$ unless $j_2=-1+j_3$. This means that the lowest energy state has $q_x=q_y=0$, then all spins in a c-plane are parallel as observed. So we consider only ε_1, ε_2 and ε_5. From the comparison of ε_1 and ε_2 we have four regions in (j_2, j_1) plane. The four regions, together with the lowest energy and the angle θ given by eq.(24) in each region, are summarized as follows:

In the case of $j_3\leqq 1$:

region 1: $j_1>2(1-j_3)$, $j_2>1-j_3$; $\varepsilon_1=-\frac{1}{2}j_1-(j_2+j_3-1)$; $\theta=0$

region 2: $j_1>-2(1-j_3)$, $j_2<1-j_3$, $j_1>2j_2$; $\varepsilon_1=-\frac{1}{2}j_1+(j_2+j_3-1)$; $\theta=\pi$

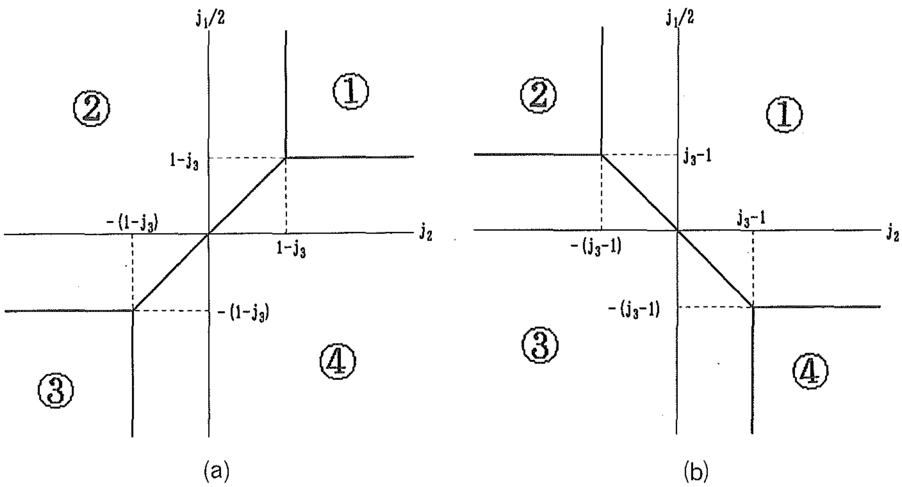

Fig. 3. Four regions in $(j_2, j_1/2)$ plane.
(a) $j_3<1$ (b) $j_3>1$

region 3: $j_1<-2(1-j_3),\ j_2<-(1-j_3)\ ;\ \varepsilon_2=\frac{1}{2}j_1+(j_2-j_3+1)\ ;\ \theta=\pi$

region 4: $j_1<2(1-j_3),\ j_2>-(1-j_3),\ j_1<2j_2\ ;\ \varepsilon_2=\frac{1}{2}j_1-(j_2-j_3+1)\ ;\ \theta=0$

Four regions in the case of $j_3<1$ are shown in Fig.3(a).

In the case of $j_3\geqq 1$:

region 1: $j_1>2(1-j_3),\ j_2>1-j_3,\ j_1>-2j_2\ ;\ \varepsilon_1=-\frac{1}{2}j_1-(j_2+j_3-1)\ ;\ \theta=0$

region 2: $j_1>-2(1-j_3),\ j_2<1-j_3\ ;\ \varepsilon_1=-\frac{1}{2}j_1+(j_2+j_3-1)\ ;\ \theta=\pi$

region 3: $j_1<-2(1-j_3),\ j_2<-(1-j_3),\ j_1<-2j_2\ ;\ \varepsilon_2=\frac{1}{2}j_1+(j_2-j_3+1)\ ;\ \theta=\pi$

region 4: $j_1<2(1-j_3),\ j_2>-(1-j_3)\ ;\ \varepsilon_2=\frac{1}{2}j_1-(j_2-j_3+1)\ ;\ \theta=0$

Four regions in the case of $j_3>1$ are shown in Fig. 3(b).

Next we compare ε_1 or ε_2 in each region with ε_5 of double helical spin arrangement. In the cases of $q=(0, 0, 0,)$ and $q=(0, 0, 2\pi/c)$, ε_5 of eq. (22e) becomes

$$\left.\begin{aligned}\varepsilon_5(q=0)&=-\frac{1}{2}j_1-|j_2+j_3-1|\\ \varepsilon_5(q=2\pi/c)&=\frac{1}{2}j_1-|j_2-j_3+1|\end{aligned}\right\}\quad(25)$$

Therefore $\varepsilon_5(q=0)$ equals ε_1 in the regions 1 and 2, and $\varepsilon_5(q=(0, 0, 2\pi/c))$ equals ε_2 in the regions 3 and 4. From these results we have found that in each region the boundary curve between the double helical spin arrangement and collinear spin

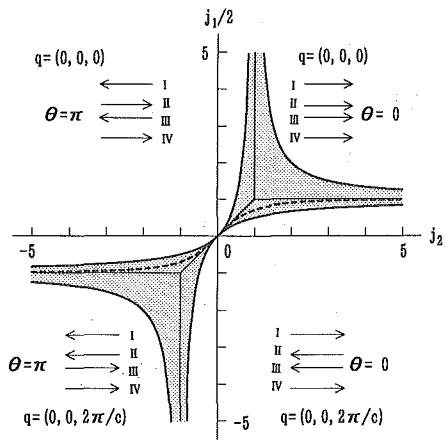

Fig. 4. Phase diagram for the case of $j_3=0$. Shaded region represents the phase with double helical spin arrangement. Four types of collinear spin arrangement, specified by the wave vector $\vec{q}$ and the relative angle θ between Cu_{II} spin and Cu_{III} spin, are described schematically. On the dotted line in the shaded region, the double helical spin arrangement with $q=(0, 0, \pi/c)$ is realized.

arrangement is given by eq. (21) with $q=0$ or $q=2\pi/c$. Then boundary curves are

$$j_1=\frac{2j_2(1-j_3)+8j_3}{j_2-(1-j_3)}=\frac{2(1+j_3)^2}{j_2-(1-j_3)}+2(1-j_3) \quad \text{in region 1} \tag{26a}$$

$$j_1=-\frac{2j_2(1-j_3)+8j_3}{j_2-(1-j_3)}=-\frac{2(1+j_3)^2}{j_2-(1-j_3)}-2(1-j_3) \quad \text{in region 2} \tag{26b}$$

$$j_1=-\frac{2j_2(1-j_3)-8j_3}{j_2+(1-j_3)}=\frac{2(1+j_3)^2}{j_2+(1-j_3)}-2(1-j_3) \quad \text{in region 3} \tag{26c}$$

$$j_1=\frac{2j_2(1-j_3)-8j_3}{j_2+(1-j_3)}=-\frac{2(1+j_3)^2}{j_2+(1-j_3)}+2(1-j_3) \quad \text{in region 4} \tag{26d}$$

In (j_2, j_1) plane, each boundary curve represents a hyperbola.

Asymptotic lines of the hyperbola of (26a) are the boundaries between regions 1 and 2, and 1 and 4, respectively. Those of (26b) are between regions 2 and 3, and 2 and 1, those of (26c) are between regions 3 and 4, and 3 and 2, and those of (26d) are between regions 4 and 1, and 4 and 3. The line $j_1=2j_2$ crosses the hyperbolae of eq. (26b) and (26d) at $j_2=\pm 2\sqrt{|j_3|}$ in the case of $j_3<0$. In the region surrounded by these branches of hyperbolae and separated by the segment connecting $(2\sqrt{|j_3|}, 4\sqrt{|j_3|})$ and $(-2\sqrt{|j_3|}, -4\sqrt{|j_3|})$, a double helical spin arrangement is most stable. The phase diagram for the case of $j_3=0$ is shown in Fig.4. Fig. 5 (a)~(f) show the phase diagram for the cases of $j_3=-0.09$, -0.25, -0.5, -1, -1.5 and -1.7, respectively. In the shaded region the double helical spin arrangement is realized. Here it should be noted that the introduction of negative j_3 enlarges the collinear region 2 with $(q=0, \theta=\pi)$ and 4 with $(q=2\pi/c, \theta=0)$, and reduces the collinear region 1 with $(q=0, \theta=0)$ and 3 with $(q=2\pi/c, \theta=\pi)$. This result is resonable because negative j_3 is favourable to antiferromagnetic arrangement between Cu_{IV} and Cu_{III} or Cu_{II} and Cu_{I}. Also, the introduction of negative j_3 narrows remarkably the region of the double helical spin arrangemnt, and for $j_3=-1$ the bouble helical region venishes completely as shown in

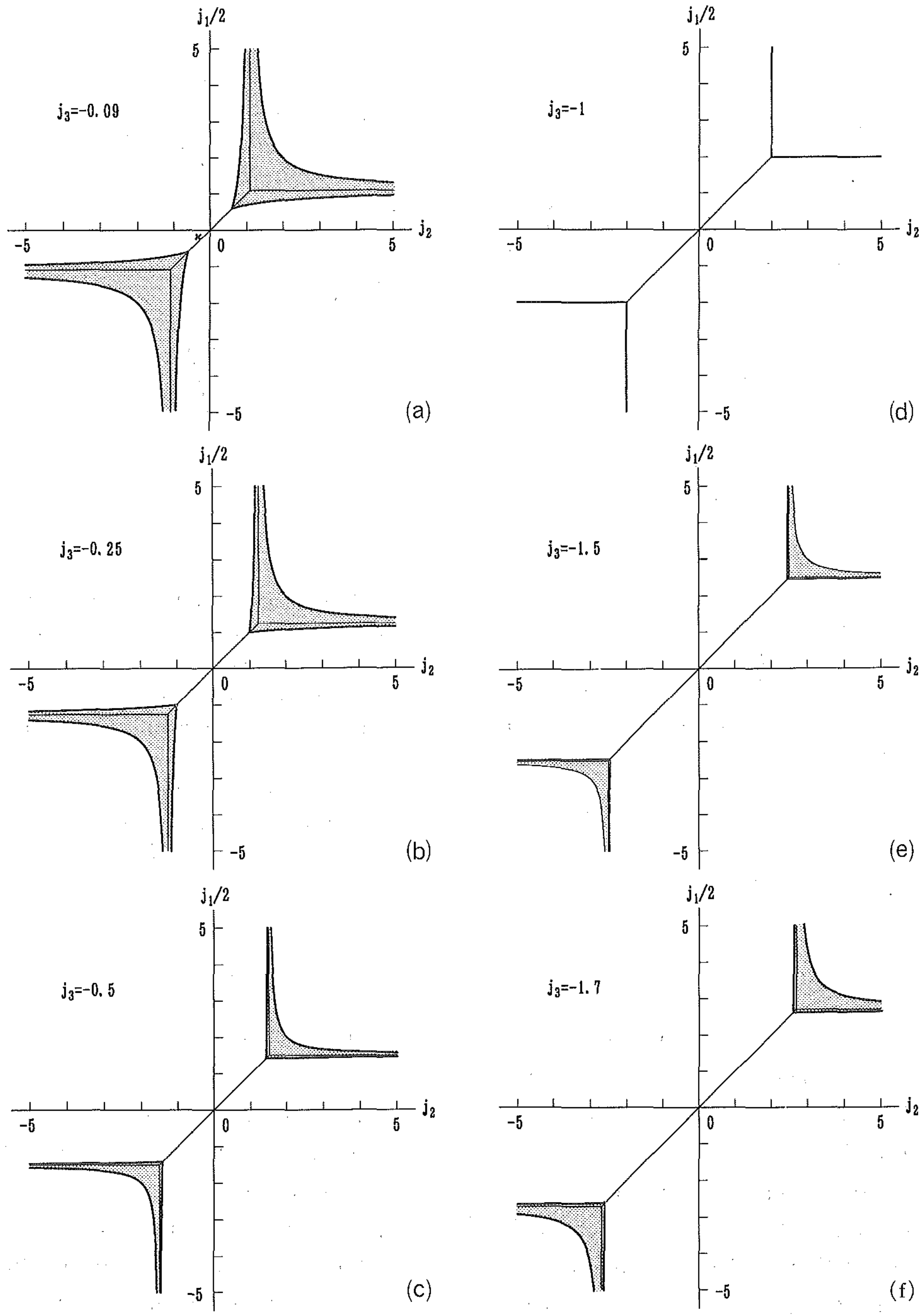

Fig. 5. Phase diagram for the cases of (a) $j_3=-0.09$, (b) $j_3=-0.25$, (c) $j_3=-0.5$, (d) $j_3=-1$, (e) $j_3=-1.5$ and (f) $j_3=-1.7$.
Shaded regions are with the double helical spin arrangement. For $j_3=-1$, the double helical region vanishes completely. The point $\times$ in (a) corresponds to the values of the exchange parameters estimated by Aïn et al, $j_1/2=-0.18$, $j_2=-0.32$ and $j_3=-0.09$.

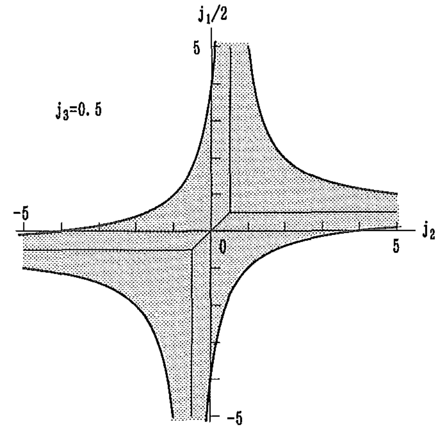

Fig. 6.

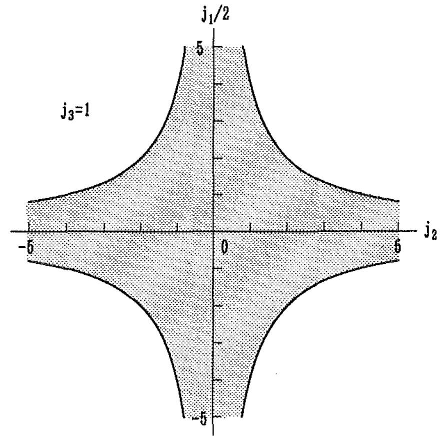

Fig. 7.

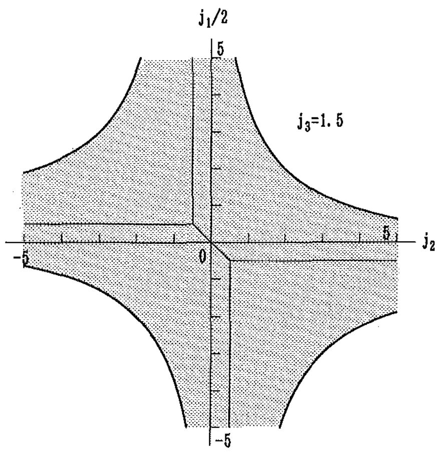

Fig. 8.

Fig. 6. Phase diagram for the case of $j_3=0.5$, shaded region being with double helical spin arrangement.

Fig. 7. Phase diagram for the case of $j_3=1.0$, shaded region being with double helical spin arrangement.

Fig. 8. Phase diagram for the case of $j_3=1.5$, shaded region being with double helical spin arrangement.

Fig. 5(d). For $j_3<-1$, the double helical region appears again and enlarges if the absolute value of j_3 increases. The line $j_1=2j_2$ crosses the hyperbolae of eq. (26b) and (26d) at $j_2=\pm 2\sqrt{|j_3|}$. In the region surrounded by the branches of hyperbolae (26a), (26b) and (26d), and the region surrounded by the branches of hyperbolae (26c), (26b) and (26d), which are separated from each other by the segment connecting $(2\sqrt{|j_3|}, 4\sqrt{|j_3|})$ and $(-2\sqrt{|j_3|}, -4\sqrt{|j_3|})$, a double helical spin arrangement is realised.

The values of J's estimated by Aïn et al[4] from their own neutron scattering data correspond to $j_1=-0.36$, $j_2=-0.32$ and $j_3=-0.09$, and the corresponding point marked by × in Fig. 5(a) lies in the collinear region 2.

Next we consider the case of $0\leqq j_3\leqq 1$. In this case the line $j_1=2j_2$ has no crossing point with the hyperbolae given by eq.(26b) and (26d). Then the double helical region is enlarged if j_3 increases toward 1. Also, by introducing positive j_3 less than 1, the collinear region 1 with ($q=0$, $\theta=0$) and 3 with ($q=2\pi/c$, $\theta=\pi$) are slightly expanded, region 2 with ($q=0$, $\theta=\pi$) and 4 with ($q=2\pi/c$, $\theta=0$) are reduced, and the double helical region is largely expanded. The phase diagram for the case of $j_3=0.5$, as an example, is shown in Fig. 6. Fig. 7 shows the phase diagram for the case of $j_3=1$.

Finally we consider the case of $j_3>1$. In Fig. 8 we show the phase diagram for the case of $j_3=1.5$, as an example. When j_3 increases, the collinear region 2 with ($q=0$, $\theta=\pi$) and 4 with ($q=2\pi/c$, $\theta=0$) are reduced, region 1 with ($q=0$, $\theta=0$) and 3 with ($q=2\pi/c$, $\theta=\pi$) are slightly expanded, and the double helical region enlarges remarkably.

References

[1] J. P. Attfield: J. Phys. Condens. Matter **1** (1989) 7045-7053.

[2] E. W. Ong, G. H. Hwei, R. A. Robinson, B. L. Ramakrishna and R. B. Von Dreele: Phys. Rev. B **42** (1990) 4255-4262.

[3] K. Yamada, K. Takada, S. Hosoya, Y. Watanabe, Y. Endoh, N. Tomonaga, T. Suzuki, T. Ishigaki, T. Kamiyama, H. Asano and F. Izumi: J. Phys. Soc. Jpn. **60** (1991) 2406-2414.

[4] M. Aïn, G. Dhalenne, O. Guiselin, B. Hennion, A. Revcolevschi; Phys. Rev. B **47** (1993) 8167-8171

[5] H. Ohta, K. Yoshida, T. Matsuya, T. Nanba, M. Motokawa, K. Yamada, Y. Endoh and S. Hosoya: J. Phys. Soc. Jpn. **61** (1992) 2921-2929.